이학석사 학위논문

Refining the source attribution estimates of $PM_{2.5}$ in Korea during KORUS-AQ using improved emissions and chemical schemes

배출 인벤토리 및 화학 스킴 업데이트를 통한 KORUS-AQ 기간 우리나라 $PM_{2.5}$ 오염원 분석 개선

2021년 08월

서울대학교 대학원

지구환경과학부

곽 병 현

Refining the source attribution estimates of $PM_{2.5}$ in Korea during KORUS-AQ using improved emissions and chemical schemes

지도교수 박 록 진

이 논문을 이학석사 학위논문으로 제출함
2021년 05월

서울대학교 대학원
지구환경과학부
곽 병 현

곽병현의 이학석사 학위논문을 인준함
2021년 07월

위 원 장 김상우

부위원장 박록진

위 원 임규호

Abstract

There are concerns on public health and air quality regarding the exposure to $PM_{2.5}$ concentration in South Korea, which is three times higher than the WHO guideline in 2015. Thus, investigating the potential emission and source regions of $PM_{2.5}$ is crucial to develop effective regulation standards. In this study, GEOS-Chem, a 3D chemical transport model, was used to simulate $PM_{2.5}$ with an updated anthropogenic emission inventory of KORUS ver.5.0 during the KORUS-AQ campaign (May-June 2016), an intercontinental cooperative air quality field study in South Korea in collaboration with the United States. Extensive ground observations at six sites (Bangnyung, Bulkwang, Gwangju, Jeju, Olympic park, and Ulsan) were used to evaluate the model performance. For further improvement, a novel SOA formation scheme was employed in the model. Overall, the simulated $PM_{2.5}$ and its tracers agree well with the observations and are enhanced compared to those of previous studies. Next, we conducted source attribution using the GEOS-Chem adjoint model under four meteorological periods during KORUS-AQ, including dynamic weather, stagnant, extreme pollution, and blocking pattern periods. There is a high contribution of domestic sources to $PM_{2.5}$ during dynamic weather, stagnant, and blocking pattern periods (about 73%, 58%, and 63%, respectively). Under strong transport conditions of the extreme pollution period, the Chinese contribution is dominant (about 57%). Considering emission sources, $PM_{2.5}$ is most sensitive to NH_3 emissions (38%) because South Korea is under NH_3-poor conditions, as verified by the adjusted gas ratio (AGR) calculation (0.53). The

contributions of organic carbon (18%), aromatics (14%), SO_2 (11%), NO_x (10%), and BC (9%) emissions follow in that order. However, there are uncertainties about the meteorological data used in the model; thus, additional adjoint analysis was conducted using GRIMs data. GRIMs shows lower temperature and higher relative humidity in South Korea, which are favorable for the chemical reactions of nitrate. The calculated AGR (0.75) also indicates that South Korea is under the NH_3-poor condition. Adjoint analysis using GRIMs shows more contribution of NH_3 (40%) and NO_x (11%) than those obtained using GEOS-FP. Additionally, meteorological effects on adjoint analysis were confirmed and quantified by MLR and LMG method, and it suggests that temperature, U wind, and RH are leading factors for domestic sources.

Keyword : KORUS ver.5.0 inventory, SOA scheme, KORUS-AQ, Source attribution, AGR, LMG method.
Student Number : 2019-29383

Table of Contents

List of Tables

List of Figures

Chapter 1. Introduction

Air pollution has immensely increased since the industrial revolution, and fine particulate matter with a diameter of less than 2.5 mm ($PM_{2.5}$) is one of the major air pollutants. In particular, $PM_{2.5}$ has adverse effects on human health, causing cardiovascular and respiratory disease and lung cancer, and long-term exposure to $PM_{2.5}$ has been associated with increased mortality (e.g., Laden et al., 2006; Krewski et al., 2009; Jerrett et al., 2009; Pellucchi et al., 2009; Pope et al., 2009; Brook et al., 2010; Lim et al., 2012; Lepeule et al., 2012).

South Korea has recorded the fastest growing economy and industry; hence, development results in conflict between increasing materials for welfare and its rebounds (Jes Fenger, 2009). This means that people suffer more from pollution than in the past because of the emissions from the combustion of fossil fuels in power plants or automobiles, biomass burning, and byproduct from industrial processes and households. Therefore, there has been an increased concern on public health, such as healthcare and policies for pollution controls (Larkin et al., 2016).

Recently, South Korea was ranked the highest population exposure to outdoor $PM_{2.5}$ among the OECD countries and 4th globally, and the $PM_{2.5}$ concentration level is about three times higher than the WHO' s air quality guidelines in 2015 (OECD, 2018). To improve air quality, the government enhanced the regulation of environmental policy in 2018, which maintains that the annual mean and 24-hour average concentration of $PM_{2.5}$

should not exceed 15 and 35 $\mu g/m^3$.

The changes in air pollutant concentrations could be influenced by the emission of their precursors (Streets et al., 2009). For $PM_{2.5}$, the major chemical components include sulfate (SO_4^{2-}), nitrate (NO_3^-), ammonium (NH_4^+), elemental carbon (EC), and organic carbon (OC) (Boming et al., 2003), and their precursors are mainly SO_2, NO_x, NH_3, EC, and OC, respectively. Factors affecting the $PM_{2.5}$ concentration in South Korea can be classified by various criteria. One of them is the origin: transported from foreign regions vs. local pollution. Next is what it is generated from: anthropogenic, natural, and biomass burning emissions. Thus, it is important to investigate the emission sector and potential sources to develop an effective air quality policy.

Studies based on modeling have employed forward sensitivity analysis for source attribution (Jeon et al., 2014; Kim et al., 2017a, 2017b), which diagnose the impacts of changing specific control parameters, such as emission. However, this approach has limitations because few emission species/sectors/regions can be evaluated in a computationally expedient manner (Choi et al., 2019). Otherwise, measurements with back trajectories and statistical source-receptor models have been widely used to identify the sources (Kang et al., 2004; Park and Kim, 2005; Kim et al., 2007; Heo et al., 2009; Choi et al., 2013; Jeong et al., 2017). Long-range transboundary air pollutants (LTP) project in Northeast Asia, which was established to investigate the mechanism of transboundary movement of pollutants in northeast Asian countries (Korea, China, and Japan) from 1996, reported fourth stage joint research focused on the source-receptor relationship of the $PM_{2.5}$ concentration over Korea,

China, and Japan in 2013-2017 (LTP, 2019). First, through intensive monitoring of air pollutants, it was obtained that sulfate, nitrate, and ammonium are the major chemical components of $PM_{2.5}$ over East Asia. Then, the source-receptor relationship of transboundary air pollution was studied through modeling.

Recently, adjoint sensitivity analysis has been employed for source attribution. It calculates the sensitivity of $PM_{2.5}$ with respect to the emissions from each species, sector, or grid cell in a single backward integration (Choi et al., 2019). For example, Lee et al. (2017) compared the observation and simulation results of $PM_{2.5}$ in Seoul in May from 2009 to 2013. Then, adjoint sensitivity analysis was conducted for the period when $PM_{2.5}$ air quality violation was observed (more than 50 $\mu g/m^3$ for 24-hour average concentration). It provided a quantitative understanding of the relative contribution of emission sources and potential source regions.

KORUS-AQ, an international cooperative air quality field study in South Korea, was conducted by the National Institute of Environmental Research (NIER), South Korea, and the United States National Aeronautics and Space Administration (NASA) in May-June 2016. The main goal of the study was to clarify the factors contributing to the air quality in South Korea. During the campaign period, detailed measurements were collected from aircraft, ground monitoring, and ships. Also, intensive observation data of $PM_{2.5}$ and related species were collected. Both local and transboundary pollution under various meteorological conditions were identified and provided, which is the best means to determine sources of $PM_{2.5}$ in South Korea.

Choi et al. (2019) investigated the emission sources and regional contribution of $PM_{2.5}$ in South Korea during the KORUS-AQ campaign through adjoint sensitivity analysis. They compared the observation and modeling results of $PM_{2.5}$ and its species using anthropogenic emission inventory from KORUS-AQ, KORUS ver.2.0 inventory. Then adjoint sensitivity analysis was conducted under four synoptic patterns: dynamic weather, stagnant, extreme pollution, and blocking pattern period. However, the simulated $PM_{2.5}$ was underestimated by 29% due to OA underestimation (Choi et al., 2019). More importantly, they found that regional contributions of $PM_{2.5}$ depend largely on meteorological conditions. To examine these issues, in this study, we conducted source attribution using the updated emission of KORUS ver.5.0 and the refined SOA formulation scheme following the VBS case study by Hodzic et al. (2016) to improve $PM_{2.5}$ estimation. In addition, we confirmed the uncertainty from meteorological data.

Chapter 2. Observations during KORUS-AQ

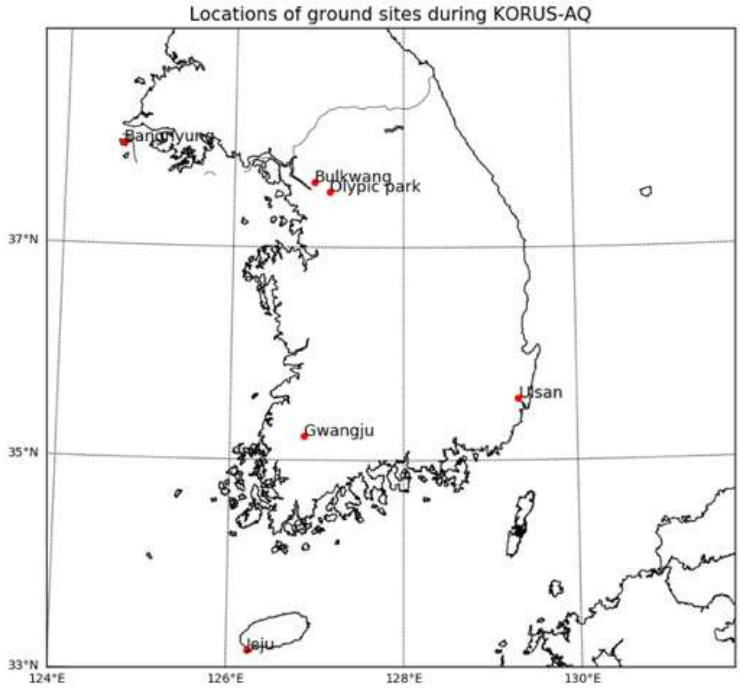

Figure 1. Locations of six ground sites (Bangnyung, Bulkwang, Gwangju, Jeju, Olympic park, and Ulsan) for the KORUS-AQ Campaign.

Observation data during the KORUS-AQ include hourly $PM_{2.5}$ and its comprising species (SO_4^{2-}, NO_3^-, NH_4^+, EC, and OC) measured at six ground sites in South Korea (**Figure 1**). These sites were selected as they are spatially distributed to represent the entire area of South Korea. Observation data at the Olympic park were measured by the Seoul Metropolitan Government Research Institute of Public Health and Environment during the KORUS-AQ, and the data for other sites were obtained by NIER. For $PM_{2.5}$ measurement, FH62C14 (Thermo Scientific, USA), a radio-metric particulate mass monitor, was used at the Olympic park and BAM-1010 (Met One Instruments, Inc., USA)

was used at other sites. To measure SO_4^{2-}, NO_3^-, and NH_4^+, MARGA ADI2080 (DOGA Limited, Turkey), a monitor for aerosols and gases in ambient air, was used at Olympic Park and AIM URG-9000D (UGR Corporation, USA), an anion and cation particle and gas system, was used at other sites. EC and OC were measured at all sites using SOCEC (Sunset Laboratory Inc., USA), a Model-4 semi-continuous OC-EC field analyzer.

During the KORUS-AQ campaign, there were various meteorological conditions. The KORUS-AQ campaign period from May to June showed higher temperatures, higher humidity, longer days, more intense sunlight, and increased emission from vegetation, which could accelerate the photochemistry, contributing to the formation of $PM_{2.5}$. In addition, KORUS-AQ did not consider episodic events, such as soil dust, which is usually problematic during winter or spring. Thus, these factors enabled the observation of the violation of air quality standards for $PM_{2.5}$ and provided a favorable expectation that local sources have a great role in determining the abundance of observed $PM_{2.5}$ than the transport from other regions.

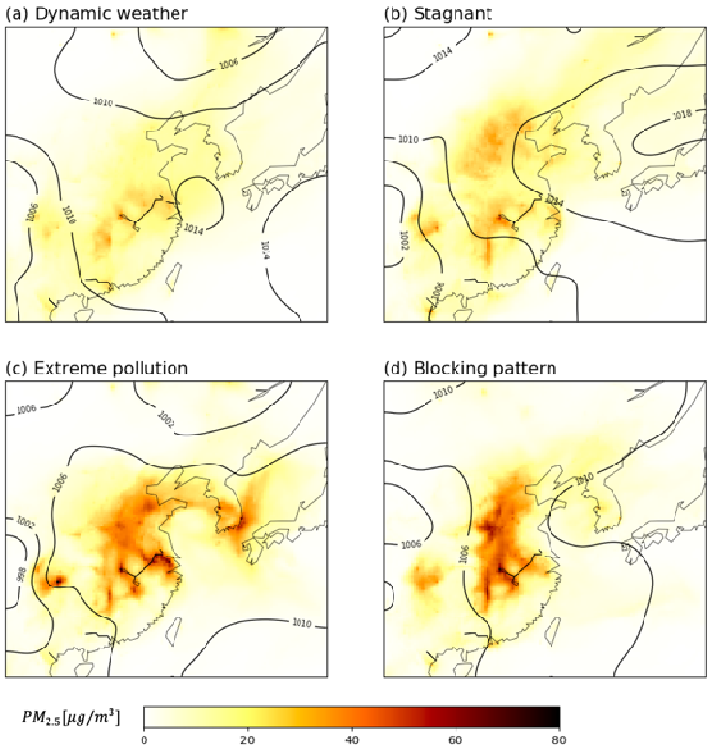

Figure 2. Mean sea level pressures (contours, hPa) and mean concentration of surface $PM_{2.5}$ (colors, $\mu g/m^3$) during each period under different meteorological conditions: (a) Dynamic weather period (May 10-16), (b) Stagnant period (May 17-22), (c) Extreme pollution period (May 25-28), and (d) Blocking pattern period (June 1-7).

Four meteorological conditions were identified during the KORUS-AQ: dynamic weather period (May 10-16), stagnant period (May 17-22), extreme pollution period (May 25-28), and blocking pattern period (June 1-7). **Figure 2** shows the simulated mean sea level pressure and concentration of $PM_{2.5}$ during each period. In the dynamic weather period, there was a rapid cycle of clear and overcast or rainy days by the frontal movements. In the stagnant period, the Korean peninsula was under the influence of a persistent anticyclone system, thus transport from

the upwind region was diverted and the air was congested. The extreme pollution period was characterized as an only observed violation of air quality standard for $PM_{2.5}$ (greater than 50 $\mu g/m^3$ for 24-hour average concentration in 2016), which showed enhanced transport from upwind regions of China with several weak cold fronts, facilitating gradual transport. The blocking pattern period showed a Rex blocking pattern through East Asia, limited transport by relatively enhanced meridional wind. Various synoptic meteorology data between periods enable the comparison of source attributions under different meteorological conditions; however, they induce uncertainty from the meteorological fields of the model.

In this study, not only source attribution was conducted for $PM_{2.5}$ in South Korea during KORUS-AQ with four meteorological conditions but also the uncertainty of the meteorological field used in the model was confirmed. In addition, $PM_{2.5}$ simulations were improved by refining the SOA formulation scheme. Its detail is discussed in Chapter 3.

Chapter 3. GEOS-Chem model simulation

GEOS-Chem is a global 3D chemical transport model for fully coupled oxidants-aerosol simulations. GEOS-Chem includes detailed tropospheric gas phase chemistry of O_3-NO_x-VOCs **(Bey et al., 2001; Hudman et al., 2007)** and externally mixed aerosols, including H_2SO_4-HNO_3-NH_3 and carbonaceous aerosols **(Park et al., 2003, 2004, 2006)**. ISORROPIAII is used for calculating the thermodynamic equilibrium between gases and aerosols **(Fountoukis and Nenes, 2007; Pye et al., 2009; Capps et al., 2012)**. Wet and dry deposition are computed using the schemes of **Liu et al. (2001)** and **Wesely (1989)**, respectively.

To simulate $PM_{2.5}$ concentration and its tracers in South Korea, a nested version of GEOS-Chem with high resolution (0.25° × 0.3125°) is used. First, a global simulation with 2° × 2.5° resolution is conducted to get the boundary conditions for the China-nested domain (11° N-55° N, 70° E-150° E). Then, the results are used for a smaller nested domain, the Northeast Asia-nested domain (20° N-50° N, 100° N-140° N). The Northeast Asia-nested domain reduces the computational costs of heavy adjoint simulations for source attribution **(Lee et al., 2017; Choi et al., 2019)**. Meteorological data is GEOS-FP, which has a resolution of 0.25° × 0.3125° with 47 vertical levels covering the Northeast Asia-nested domain.

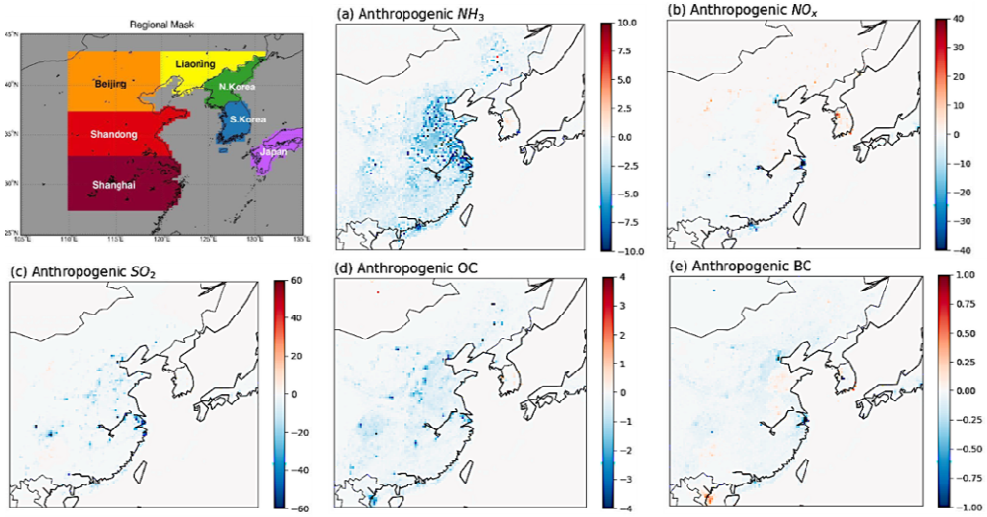

Figure 3. Spatial distribution of the difference between KORUS ver.5.0 inventory and KORUS ver.2.0 inventory for anthropogenic (a) NH_3, (b) NO_x, (c) SO_2, (d) OC, and (e) BC emission. Units are Gg/year.

Table 1. Relative difference (%) of anthropogenic NH_3, NO_x, SO_2, OC, and BC emission in each region. Eastern China consists of Shanghai, Shandong, Beijing, Liaoning region, South Korea is S. Korea, and other consists of N. Korea and Japan like in "Regional Mask" in **Figure 3**.

	NH_3	NO_x	SO_2	OC	BC
Eastern China	45% ▼	7% ▼	42% ▼	54% ▼	24% ▼
South Korea	17% ▼	37% ▲	7% ▼	133% ▲	–
Other	10% ▼	13% ▲	47% ▼	25% ▼	33% ▼

The KORUS emission inventories were developed based on the Comprehensive Regional Emissions inventory for Atmospheric Transport Experiment **(Woo et al., 2012)**. KORUS ver.5.0 inventory was initially developed based on the updated emissions for Korea (Clean Air Policy Support System, CAPSS, 2015), China (Multiresolution Emission Inventory for China, MEIC, 2016), and Japan ($PM_{2.5}$ EI 2015). Then, it was adjusted continuously based on feedback from the observations and

modeling. In more detail, NO_x emissions in South Korea increased by 37%. It reflects the findings of satellite-based top-down analysis by **Goldberg et al. (2019)** and **Miyazaki et al. (2019),** where NO_2 values are 1.37 times larger in the Seoul metropolitan area than bottom-up emission inventories, and NO_x emission is 40% higher than KORUS v2 inventory in South Korea, respectively.

Biomass burning emissions are from GFED3 monthly data (Giglio et al., 2010), and biogenic emissions are from MEGAN **(Guenther, 2006)**. NO_x emissions from natural sources, including the soil **(Yienger and Levy, 1995; Wang et al., 1998)** and lightning **(Murray et al., 2012),** are used. Natural emissions of NH_3 are from GEIA **(Bouwmann et al., 1997)**.

Additionally, diurnal variations of NH_3 emissions following **Zhu et al. (2015)** and **Lee et al. (2017)** are applied to model and photolysis of particulate nitrate, which is a major source of daytime HONO and NO_x **(Ye et al., 2016)** and can be an additional loss of nitrate in the daytime, is applied to the model simulation.

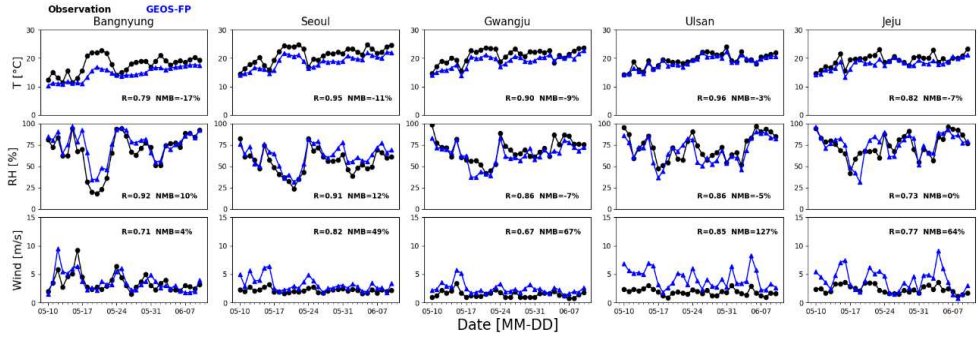

Figure 4. Daily averaged temperature (° C), relative humidity (%), and wind speed (m/s) at five ground sites during the KORUS-AQ (May 10-June 10). Black circles are observations and blue triangles are from GEOS-FP meteorological field.

Before evaluating the performance of the forward model, the meteorological data are validated. GEOS-FP is an assimilated meteorological data from the Goddard earth observing system (GEOS) of the NASA global modeling and assimilation office. **Figure 4** compares the daily average temperature, relative humidity, and wind speed between the GEOS-FP meteorological data and in situ observations at five sites: Bangnyung, Seoul, Gwangju, Ulsan, and Jeju. The observation data were provided by Korea Meteorological Administration. Temperature and relative humidity from GEOS-FP show good agreement with the observations; however, GEOS-FP overestimates wind speed at all regions.

Equation (1) AROM + OH → ARO2
Equation (2) ARO2 + NO → LARO2N
Equation (3) ARO2 + HO_2 → LARO2H
Equation (4) SOA = α * (LARO2N + LARO2H) * γ
Equation (5) γ = SOA / (SOA + SOG)

The standard GEOS-Chem adjoint model does not simulate SOA; thus, OA is significantly underestimated. To solve this issue, **Choi et al. (2019)** added a simple SOA formation scheme from aromatic species (benzene, toluene, and xylene), as shown in **Equations (1)-(5),** to the GEOS-Chem adjoint model to reduce the difference between the simulated and observed OA concentrations. AROM and ARO2 indicate anthropogenic aromatics species and their oxidation products, respectively, LARO2N and LARO2H are intermediate species from the oxidation of ARO2 by NO and HO_2, respectively **(Choi et al.,**

2019), and α is a gas phase SOA yield parameter, thus α * (LARO2N + LARO2H) is a secondary organic gas phase product (SOG). The formation of SOG is based on Jo et al. (2013), which implements chemical aging in GEOS-Chem using the VBS approach, and α values corresponding to each volatility bins are obtained from laboratory measurements by Ng et al. (2007). γ is the ratio to convert SOG to SOA, and it is calculated by average budgets of SOG and SOA within Northeast Asia-nested simulation during KORUS-AQ.

Table 2. Alpha values by volatility cases from Choi et al. (2019) (Base) and Hodzic et al. (2016) (Updated).

		C*	0.01	0.1	1	10	100	1000
High-NOx	BENZ	Base			0.0778	0	0.7932	
		Updated	0.031	0.011	0.507	0.019	0.03	0.142
	TOLU	Base			0.0315	0.0944	0.08	
		Updated	0.042	0.123	0.263	0.02	0.319	0.329
	XYLE	Base			0.025	0.036	0.0899	
		Updated	0.015	0.056	0.006	0.026	0.087	0.193
Low-NOx	BENZ	Base	0.37					
		Updated	0.007	0.003	0.27	0.142	0.4	0.12
	TOLU	Base	0.3					
		Updated	0.371	0.028	0.207	0.586	0.063	0.138
	XYLE	Base	0.36					
		Updated	0.395	0.041	0.203	0.121	0.232	0.145

However, γ was still underestimated by 52% with little SOA formation. Therefore, α and γ values are updated to improve the SOA formation scheme with KORUS ver.5.0 anthropogenic emission inventory. First, α values are updated, as shown in Table 2, following the VBS study by Hodzic et al. (2016), which uses six-product parameterization for the further aging reaction of aromatics and results in higher yields and formation of less volatile organic species (Hodzic et al., 2016). Second, γ value is updated following model results of Yujin Oak (personal communication), which simulates SOG and SOA in Northeast Asia

domain during KORUS-AQ using GEOS-Chem v12 with KORUS ver.5.0 emission and is calculated as 0.9853.

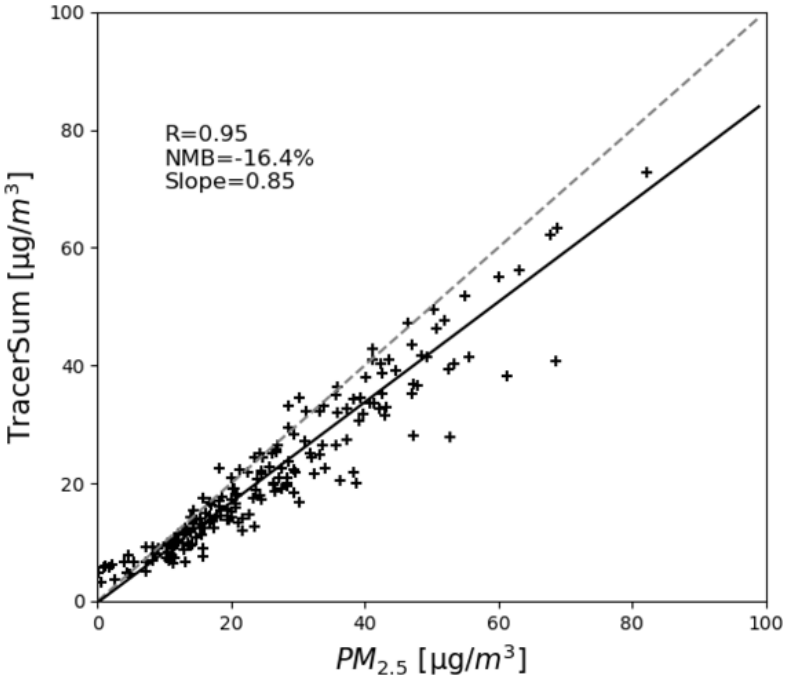

Figure 5. Daily average $PM_{2.5}$ concentration at six ground sites during KORUS-AQ. The x-axis is the observed $PM_{2.5}$ and the y-axis is the tracer sum of SO_4^{2-}, NO_3^-, NH_4^+, EC, and 2.1*OC.

The simulated $PM_{2.5}$ is defined as the sum of SO_4^{2-}, NO_3^-, NH_4^+, BC, 2.1*OC, and SOA. The factor, 2.1, is a conversion factor used to convert primary OC (POC) to primary organic aerosol following the **Turpin and Lim (2001)** recommendation to consider nonurban regions and a global mean value as recommended by GEOS-Chem Aerosol WG.

Figure 5 shows the daily average observed $PM_{2.5}$ (x-axis) and the sum of the tracers (y-axis) concentration as defined before in the six ground sites during KORUS-AQ. The correlation

coefficient between TracerSum and $PM_{2.5}$ is 0.95, and TracerSum is lower than $PM_{2.5}$ by 16.4%. This discrepancy is caused by the absence of crustal elements, such as mineral dust (Sajeev et al., 2017). Although TracerSum is the best tool to evaluate forward models due to the same definition of $PM_{2.5}$, the measured $PM_{2.5}$ has fewer missing data (16) than that of TracerSum (48), a total of 192 (32 days × 6 sites). Thus, the measured $PM_{2.5}$ is used to evaluate the forward model.

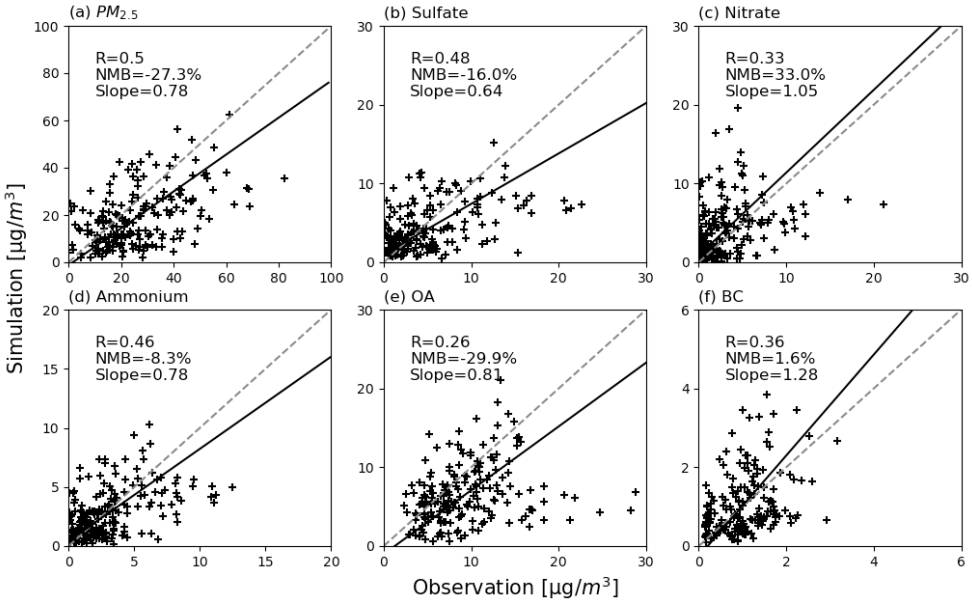

Figure 6. Scatter plots of daily average (a) $PM_{2.5}$, (b) Ammonium, (c) Sulfate, (d) Nitrate, (e) OA, (f) BC at six ground sites of Korea during KORUS-AQ (May 10-June 10) between the observation (x-axis) and model result (y-axis).

Figure 6 compares the observation and simulation results for $PM_{2.5}$ and its comprising tracers. The simulation results for sulfate, ammonium, and BC agree well with observation results, but those for nitrate and OA show some discrepancy with the

observations. Although the diurnal variations of NH_3, nitrate photolysis, and SOA formation with additional aromatic oxidation that can reduce nitrate concentrations are applied, the simulated nitrate is overestimated by 33%. The simulated $PM_{2.5}$ is also underestimated by 27.3%, which is caused by the lack of crustal elements and OA underestimation.

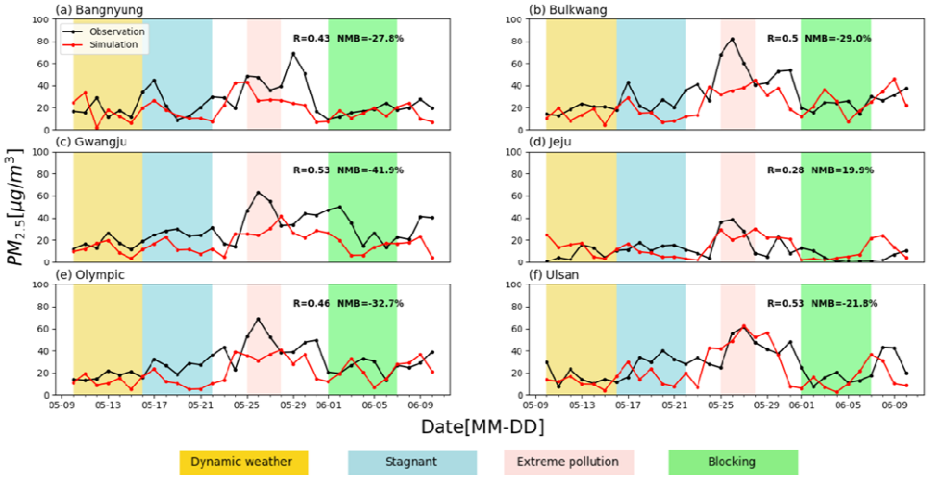

Figure 7. Daily average $PM_{2.5}$ concentration at six ground sites during KORUS-AQ, May 10-June 10. Black and red circles indicate observed and simulated $PM_{2.5}$, respectively. Each colored shading means four periods under different meteorological conditions: yellow: dynamic weather period (May 10-16); blue: stagnant period (May 17-22); pink: extreme pollution period (May 25-28); green: blocking pattern period (June 1-7).

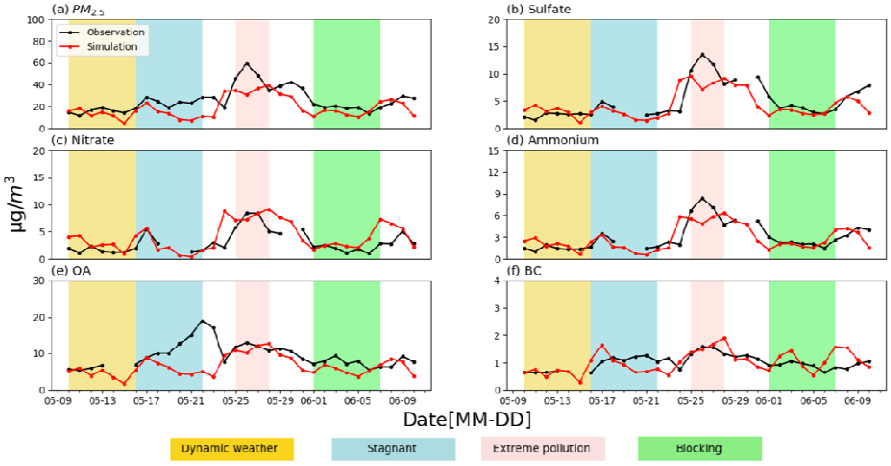

Figure 8. Daily average $PM_{2.5}$ concentration at six ground sites and its comprising tracers during KORUS-AQ, May 10-June 10. Black and red circles indicate the observed and simulated $PM_{2.5}$, respectively. Each colored shading means four periods under different meteorological conditions as in **Figure 7**.

Figure 7 compares the observed and simulated $PM_{2.5}$ at the six ground sites during KORUS-AQ. The simulated results are in good agreement with the observation results with a moderate correlation (0.28-0.53). However, the $PM_{2.5}$ concentration is severely underestimated at end of the stagnant period (May 20-24) in all regions, which is attributed to the failure to capture some pollution in South Korea. Siberian fire on May 18 reached the Korean peninsula **(Lamb et al., 2018)** and released aged smoke plumes containing additional SOA precursors **(Peterson et al., 2019)**. Monthly GFEDv3 biomass burning emission inventory, which could not capture the event, and GEOS-Chem adjoint model with simple SOA formation scheme from only aromatic species underestimated SOA in that period (**Figure 8**), which shows daily and sites average concentration of $PM_{2.5}$ and its tracers. During the extreme pollution period (pink area),

observed relative humidity (RH) was above 60% in all regions (**Figure 4**). This condition provides a favorable environment for chemical reactions that produce secondary aerosols, including secondary inorganic aerosols (e.g., sulfate, nitrate, and ammonium) and SOA **(Fu and Chen, 2017; Liu et al., 2018; Peterson et al., 2019)**. However, the adjoint model could not estimate the sustainable formation of these aerosols, especially sulfate and ammonium, as shown in **Figure 8.**

Equation (6) $$\lambda_{E,Site,Period} \equiv \frac{\partial J_{Site,Period}}{\partial E} * \frac{E}{J_{Site,Period}} * 100\,[\%]$$

Equation (7) $$J_{Site,Period} = \frac{1}{M} * \sum_{i=1}^{N} \sum_{j=1}^{M} C_{i,j}$$

For source attribution of $PM_{2.5}$ in South Korea, GEOS-Chem adjoint v35m (Henze et al., 2007) is used to calculate the adjoint gradients and model response with respect to the control parameters. Here, normalized adjoint sensitivity is calculated with respect to the emissions from each species and grid cell using **Equation (6)**, where E is the emission of each $PM_{2.5}$ precursor in a grid cell and J is the model response called the cost function. The cost function is expressed by **Equation (7),** where M is the number of days in each period under different meteorological conditions, N is the number of tracers comprising $PM_{2.5}$ (SO_4^{2-}, NO_3^-, NH_4^+, BC, OC, and SOA), and C_{ij} is the daily average concentration of aerosols comprising $PM_{2.5}$ on the surface. Here, 20 cost functions are defined, each being the average surface $PM_{2.5}$ concentration of grid cell of five ground sites (Bulkwang, Gwangju, Jeju, Olympic park, and Ulsan) in each of the four periods (dynamic weather, stagnant, extreme pollution, and

blocking pattern) in KORUS-AQ.

Equation (8) $\lambda = \frac{\partial J}{\partial \sigma}$

Equation (9) $\Lambda = \frac{J(\sigma + \delta\sigma) - J(\sigma - \delta\sigma)}{2\delta\sigma}$

Equation (10) $\Lambda = \frac{J(\sigma + \delta\sigma) - J(\sigma)}{\delta\sigma}$

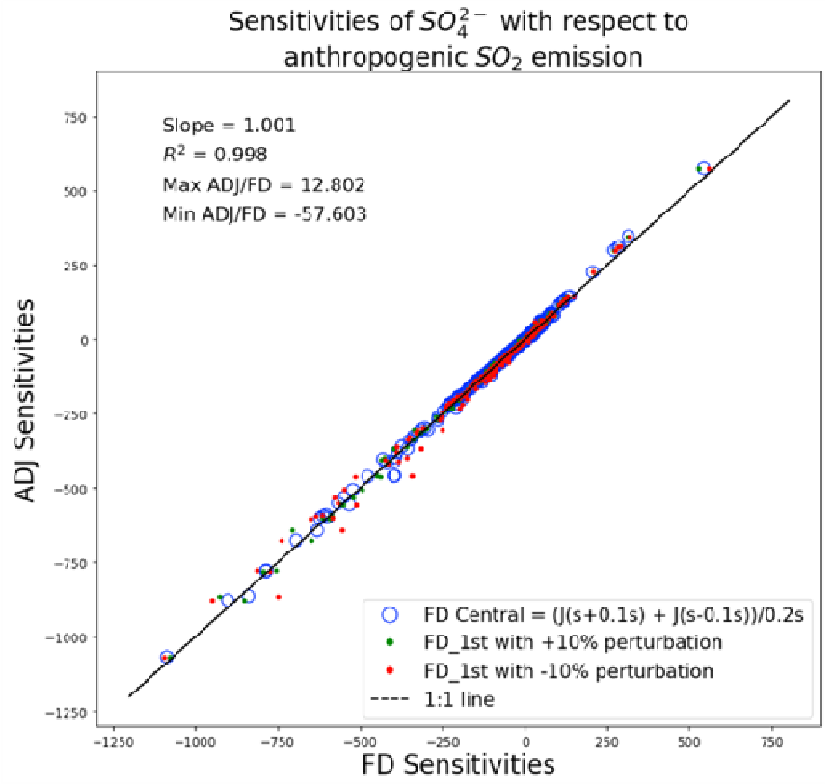

Figure 9. Scatter plot of finite difference sensitivity to the adjoint sensitivity of SO_4^{2-} with respect to anthropogenic SO_2 emissions. Blue open circles indicate the central finite difference, green and red points indicate +10% and −10% perturbation of first order finite difference, respectively.

The accuracy of the adjoint model can be tested by comparing the adjoint gradients to the finite difference gradients (Henze et

al., 2007). Equation (8) expresses the adjoint gradient, which is the model response to control parameters, such as emission. Equations (9) and (10) are the central and first order finite difference gradients, respectively, which approximate continuous adjoint gradients to discrete gradients using the finite difference method. The validation of the adjoint model is confirmed by comparing the adjoint gradients with the central and first order finite difference gradients with 10% perturbation. Figure 9 shows the result of the finite difference test. All the central finite difference gradients are located within 10% perturbation, confirming that the adjoint model is valid (Henze et al., 2007).

Chapter 4. Source attribution

$$\text{Equation (11)} \quad \lambda_{Period} = \frac{\sum_{Site}(\sum_{E}\lambda_{E,Site,Period} * Weight_{Site,Period})}{\sum_{Site} Weight_{Site,Period}}$$

$$\text{Equation (12)} \quad Weight_{Site,Period} = J_{Site,Period} * Population_{Site}$$

$$\text{Equation (13)} \quad \lambda_{E} = \frac{\sum_{Site,Period}(\lambda_{E,Site,Period} * Weight_{Site,Period})}{\sum_{Site,Period} Weight_{Site,Period}}$$

An adjoint analysis is conducted for source attribution to $PM_{2.5}$ of South Korea. First, normalized adjoint sensitivities are calculated using **Equation (6)**. After calculating the normalized sensitivities of the cost functions, the total contribution from all emission sources is estimated using **Equations (11), (12), and (13)**, considering the population exposed to $PM_{2.5}$ in South Korea in each of the four meteorological conditions. These are calculated from a specific day in each episode to the 5th day of forcing time. is the total contribution from all emission sources to $PM_{2.5}$ exposure to the population in South Korea in each meteorological period. is a weighting factor considering the population of the city where observation sites are located. Population data are obtained from the Korean Statistical Information Service census for 2015. Half of the population of Seoul is assigned to Bulkwang site to represent Gangbuk region and another to Olympic park site to represent Gangnam region, and Bangnyung site is excluded from the analysis owing to the very small population. is the contribution of each emission source to $PM_{2.5}$ exposure to the population in South Korea in the

entire period of KORUS-AQ. To compare regional contributions, eight source regions (South Korea, North Korea, Liaoning, Beijing, Shandong, Shanghai, Japan, and the rest of the domain) are defined using Regional Mask, as shown in **Figure 3.**

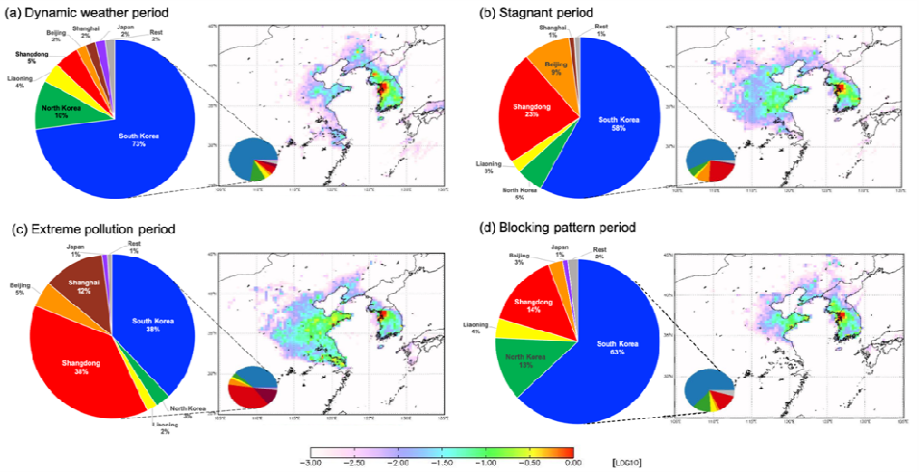

Figure 10. Regional contribution of all emission sources to $PM_{2.5}$ in South Korea in the (a) dynamic weather, (b) stagnant, (c) extreme pollution, and (d) blocking pattern periods. See **Figure 3** for the Regional Mask for each source region and color indications.

Table 3. Regional contribution to population exposure to $PM_{2.5}$ in South Korea in different periods (%) (Choi et al. 2019).

	Dynamic weather	Stagnant	Extreme Pollution	Blocking
South Korea	50	34	26	57
North Korea	6	4	3	9
Liaoning	6	2	2	3
Beijing	9	16	10	6
Shandong	17	39	38	17
Shanghai	6	2	18	~0
Japan	2	~0	~0	2
Rest of domain	4	2	2	6

Figure 10 shows the regional contribution of all emission

sources to population exposure to $PM_{2.5}$ in South Korea in four meteorological periods as calculated using **Equation (11)**. In the dynamic weather period, the domestic contribution increases by 73% compared to the results in previous studies, which is 50% in **Table 3**. In the stagnant period, the domestic and Chinese contributions account for 58% and 36%, respectively, which oppose prior studies. This discrepancy is attributed to the Siberian fire events described in **Section 2**, and prior studies also acknowledged this underestimation. Although the GEOS-Chem adjoint model could not capture the influence of the event, it is slightly resolved indirectly using the KORUS ver.5.0 inventory, which corresponds to the meteorological features of the stagnant period. In the extreme pollution period, domestic sources contribute about 38%, but Chinese regions contribute about 57%. The domestic contribution is slightly increased compared to that in previous studies. Lastly, in the blocking pattern period, domestic sources play a substantial role (65% contribution), which is similar but higher than that in prior studies.

These changes in pattern are partially attributed to the emission inventory update, which is shown in **Table 1**. In other words, the anthropogenic NH_3, SO_2, and BC emissions in eastern China relatively decrease more than those in South Korea. NO_x and OC emissions in South Korea are increased, whereas that in eastern China are decreased. These differences affect the source attribution of this study regarding the increasing contribution of domestic sources compared to the results of prior studies. Additionally, this adjoint sensitivity analysis largely depends on forward simulations, which show improvement in OA, BC, and

nitrate but more bias in ammonium and sulfate compared with prior studies. Thus, changes in emission inventory and forward simulation affect the adjoint sensitivity analysis.

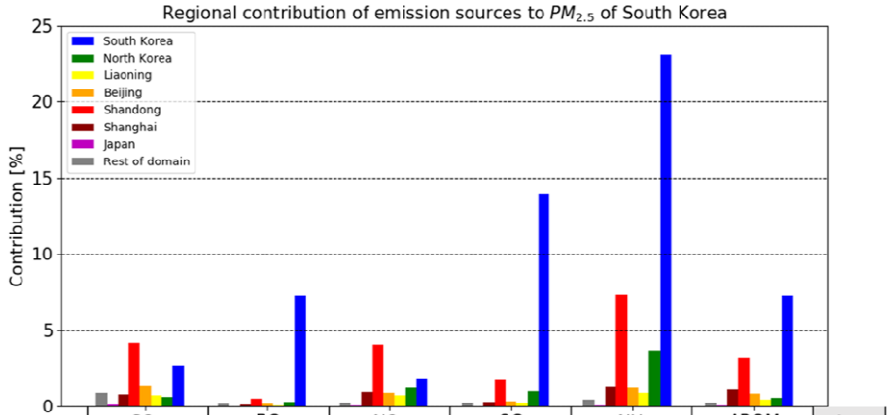

	SO_2	BC	NO_x	OC	NH_3	AROM	Sum
South Korea	2.6	7.3	1.8	13.9	23.1	7.2	55.9
North Korea	0.6	0.3	1.2	1.0	3.6	0.5	7.2
Liaoning	0.7	0.1	0.7	0.2	0.9	0.5	3.1
Beijing	1.3	0.1	0.9	0.3	1.2	0.8	4.6
Shandong	4.1	0.5	4.1	1.7	7.3	3.1	20.8
Shanghai	0.7	0.1	0.9	0.3	1.2	1.1	4.3
Others	1.0	0.2	0.3	0.2	0.5	0.3	2.5
Sum	11.0	8.6	9.9	17.6	37.8	13.5	98.4

* Others = Japan + Rest of domain

Figure 11. Regional contribution of each emission source to $PM_{2.5}$ in South Korea (%). Each color indicates different source regions. See **Figure 3** for source regions and color indications.

Figure 11 shows the regional contribution of each emission source to $PM_{2.5}$ in South Korea in a four-period average using as calculated using **Equation (13)**. The population exposed to $PM_{2.5}$ in South Korea is most sensitive to NH_3 emissions and OC, aromatic species, SO_2, NO_x, and BC in that order. However, NH_3 contributes more than 1.5 times the SO_2 and NO_x emissions. To clarify this phenomenon, the degree of sulfate neutralization and adjusted gas ratio (AGR) are calculated to determine whether South Korea is NH_3-rich or NH_3-poor. In **Equation (15)**, [TA],

[TN], and [TS] are the total molar concentration of ammonia ($[NH_3]$ + $[NH_4^+]$), nitrate ($[NO_3^-]$ + $[HNO_3]$), and sulfate ($[SO_4^{2-}]$), respectively (Wang et al., 2011).

Equation (14) $$DSN = \frac{[NH_4^+] - [NO_3^-]}{[SO_4^{2-}]}$$

Equation (15) $$AGR = \frac{[TA] - DSN * [TS]}{[TN]} = \frac{[NH_3] + [NO_3^-]}{[NO_3^-] + [HNO_3]}$$

If AGR is greater than 1, the region is NH_3-rich, which implies abundant free NH_3. The AGR for South Korea is obtained to be 0.53 using the adjoint model, which indicates that South Korea is NH_3-poor. It means that nitrate and sulfate aerosols are more sensitive to NH_3 emission than their precursor gases. Thus, the nitrate concentration can be increased, replacing the decreased sulfate (Jo et al., 2020). The results of the forward model (Figure 6) also show that nitrate is highly overestimated (NMB +33%) and sulfate is underestimated (NMB −16%). Wang et al. (2016) investigated the sources of nitrate aerosols in Northeast Asia and suggested that nitrate aerosols are generally most sensitive to NH_3 emissions in South Korea in April and July based on the calculated AGR. Moreover, Hou et al. (2019) and Pan et al. (2020) measured the regional and emission contributions to $PM_{2.5}$ in the Peral River Delta regions of China, which are representative NH_3-poor regions. They reported that the contribution of NH_3 to $PM_{2.5}$ is higher than that of the summation of other gases (SO_2 and NO_x) on average.

Based on the prior studies and adjoint analysis results, NH_3 is a key emission source that can significantly affect $PM_{2.5}$ in South Korea by not only its mass but also enhancing the nucleation of

SO_2 and NO_x to form sulfate and nitrate aerosols. In particular, domestic emissions of NH_3 account for 60% of the total contribution. This implies that regulating the emissions is the best way to reduce population exposure to $PM_{2.5}$ in South Korea. Moreover, domestic OC and aromatic species also have significant effects on the $PM_{2.5}$ concentration, but there are still uncertainties about their chemical reactions in the atmosphere. There is, therefore, a need for further studies and analyses to effectively regulate their emissions in South Korea.

Chapter 5. Discussion

Adjoint analyses are highly influenced by their meteorological conditions; therefore, KORUS-AQ was divided into four periods based on the atmospheric features. However, meteorological data used in the model can induce some uncertainties about temperature, wet/dry deposition, transport or congestion, aerosol mixing, etc., depending on which is used. Accordingly, further adjoint analyses with different meteorological data are needed to examine how those uncertainties affect the results of the forward and backward models. Global/regional-integrated model system (GRIMs) data, provided by online simulation at multiple scales **(Hong et al., 2013)**, are used for this further analysis.

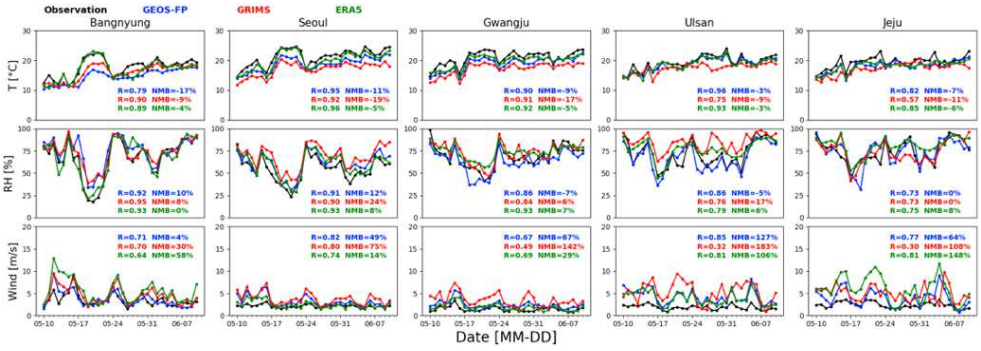

Figure 12. Daily averaged temperature (° C), relative humidity (%), and wind speed (m/s) at five ground sites during KORUS-AQ (May 10-June 10). Black circles indicate observation data, blue, red, and green circles indicate data from the GEOS-FP, GRIMs, and ERA5 ensemble mean, respectively.

Figure 12 compares the daily average temperature, RH, and wind speed between the GEOS-FP, GRIMs, and ERA5 ensemble mean data, and in situ observations for five sites: Bangnyung, Seoul, Gwangju, Ulsan, and Jeju. GRIMs data show relatively

more overestimation of temperature or underestimation of RH at Seoul, Gwangju, Ulsan, and Jeju. However, GRIMs highly overestimates wind speed at all sites. Thus, lower temperature and higher RH can enhance chemical reactions, especially for nitrate, but this can be partially compensated for with more dilution of aerosols. Additionally, ERA5 ensemble mean data from ECMWF (European Centre for Medium-Range Weather Forecasts) is used to evaluate own errors of meteorological fields. ERA5 shows similar or better results with GEOS-FP in temperature and RH, but GRIMs shows worse results among meteorological fields. In wind speed, all of data shows overestimation, which is commonly shown in most of meteorological fields, but both of ERA5 and GEOS-FP show better results than GRIMs.

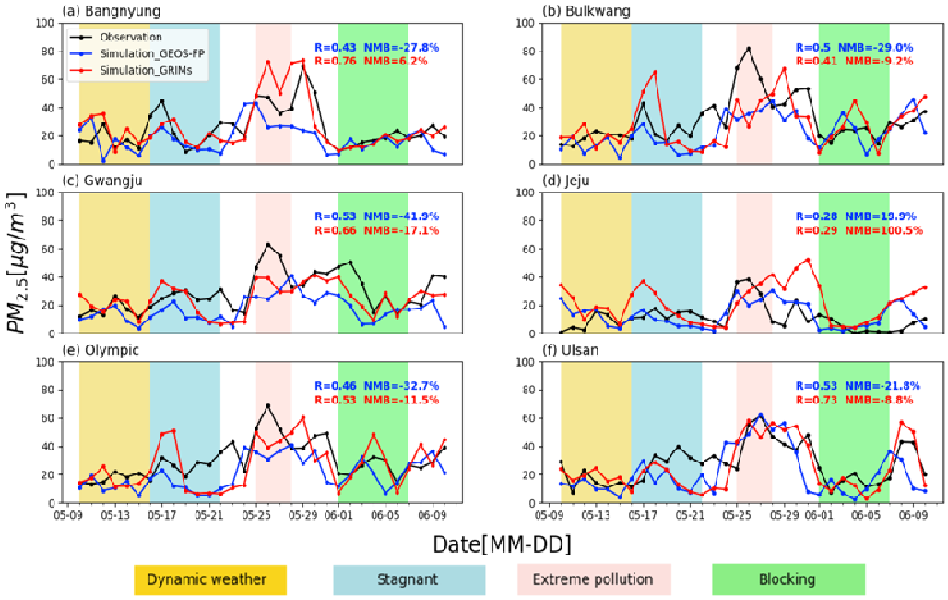

Figure 13. Daily average $PM_{2.5}$ at six ground sites during the KORUS-AQ (May 10-June 10). Black, blue, and red circles indicate observed $PM_{2.5}$, $PM_{2.5}$ simulated using GEOS-FP data, and that simulated using the GRIMs data, respectively. Shaded regions indicate four periods under different meteorological conditions: yellow—dynamic weather period (May 10-16); blue—stagnant period (May 17-22); red—extreme pollution period (May 25-28); green—blocking pattern period (June 1-7).

In **Figure 13**, the simulated $PM_{2.5}$ from GRIMs shows a higher $PM_{2.5}$ concentration in all regions than that simulated using GEOS-FP. However, the $PM_{2.5}$ simulated using GRIMs shows awkward peak concentrations in a specific period. In that period, GRIMs shows more favorable conditions for chemical reactions than GEOS-FP, including lower temperature and higher RH. These conditions can result in a peak concentration of $PM_{2.5}$.

Before conducting adjoint analyses, AGR was calculated using the GRIMs data. The AGR in South Korea is 0.75, which is higher than 0.53 from the GEOS-FP results. It means that South

Korea is closer to NH_3-rich conditions and shows less sensitivity of NH_3 emissions to sulfate and nitrate aerosols than when GEOS-FP is used. However, GRIMs shows more favorable conditions for enhancing nitrate formation. However, there can be changes in the contribution of NH_3 and NO_x emissions.

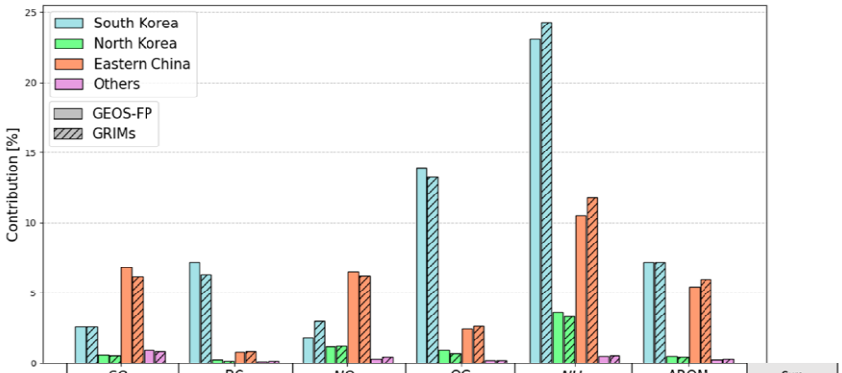

	SO_2	BC	NO_x	OC	NH_3	AROM	Sum
South Korea	2.6 (2.6)	6.4 (7.3)	3.0 (1.8)	13.2 (13.9)	24.3 (23.1)	7.3 (7.2)	**56.8 (55.9)**
North Korea	0.6 (0.6)	0.2 (0.3)	1.2 (1.2)	0.7 (1.0)	3.3 (3.6)	0.5 (0.5)	**6.5 (7.2)**
Eastern China	6.2 (6.8)	0.8 (0.8)	6.3 (6.6)	2.7 (2.5)	11.8 (10.6)	6.0 (5.6)	**33.8 (32.8)**
Others	0.9 (1.0)	0.2 (0.2)	0.5 (0.3)	0.3 (0.2)	0.6 (0.5)	0.3 (0.3)	**2.8 (2.5)**
Sum	**10.3 (11.0)**	**7.6 (8.6)**	**11.0 (9.9)**	**16.9 (17.6)**	**40.0 (37.8)**	**14.1 (13.5)**	**99.9 (98.4)**

* Data: GRIMs (GEOS-FP)

* Eastern China = Liaoning + Beijing + Shandong + Shanghai

* Others = Japan + Rest of domain

Figure 14. Regional contribution of each emission source to $PM_{2.5}$ of South Korea (%). Each color indicates different source regions: Sky blue for South Korea, light green for North Korea, orange for Eastern China, and purple for other regions. Solid bars indicate the result from GEOS-FP and hatched bars indicate the result from GRIMs. Texts inside brackets indicate contribution calculated using GEOS-FP and those outside brackets indicated those calculated using GRIMs data.

Figure 14 compares the regional contributions calculated using GEOS-FP and GRIMs data for each emission source. For better visualization to compare, the contributions from regions in eastern China are added up and colored as orange. South Korea is indicated by sky blue, North Korea by light green, and other regions, which combine Japan and the rest of the domain, by purple. With GRIMs, the regional contributions are similar, with

differences of less than 1%. However, considering emission sources, NH_3 and NO_x show more contributions to $PM_{2.5}$ (about 2%). The favorable condition for nitrate aerosols (low temperature and high RH) in South Korea results in more contribution of NH_3 and NO_x still under NH_3-poor conditions, which is calculated as 0.75 in AGR.

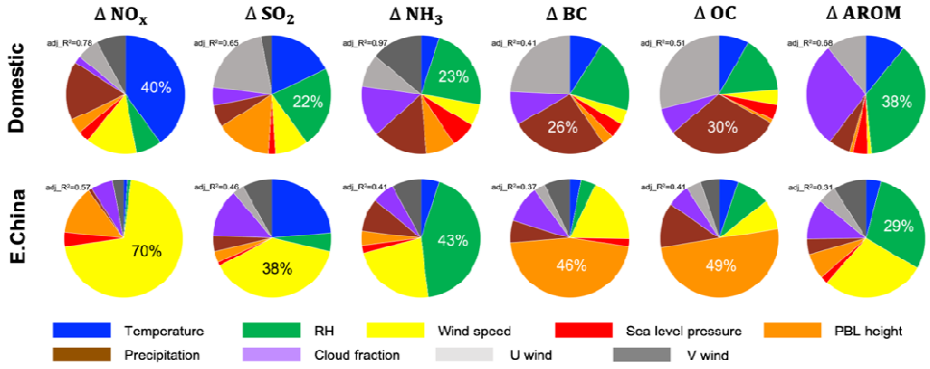

Figure 15. Relative importance of meteorological variables which influence to sensitivity of emission sources (NO_x, SO_2, NH_3, BC, OC, and AROM) to $PM_{2.5}$. Temperature, RH, Wind speed, Sea level pressure, PBL height, Precipitation, and Cloud fraction are colored as blue, green, yellow, red, orange, brown, violet, respectively.

Equation (16) $$y_i = \beta_0 + \beta_{i,1}x_{i,1} + \beta_{i,2}x_{i,2} + \cdots + \beta_{i,n}x_{i,n} + \epsilon$$

Equation (17) $$LMG(x_k) = \frac{1}{p!}\sum_{S\,Permuation} seqR^2(x_k|S)$$
$$seqR^2(x_k|S) = R^2(x_k \cup S) - R^2(S)$$

To confirm influences of these meteorological variable changes, multiple linear regression model and the LMG (Lindeman, Merenda, and Gold) method **(Groemping, 2006)** are used for each of seven meteorological variables in explaining sensitivity

change of $PM_{2.5}$ to emission sources. Multiple linear regression model of **Equation (16)** is used for correlation, where are difference of sensitivities of $PM_{2.5}$ to emission sources (), are the ensemble of meteorological variables, and are regression coefficients. The LMG method can partition total R^2 into individual R^2 contribution from each parameter like **Equation (17)**. **Figure 15** shows relative importance of meteorological variables to sensitivity change of $PM_{2.5}$. This result suggests that temperature changes are leading factor for sensitivity differences to domestic NO_x (R^2=0.78) and SO_2 (R^2=0.65) emissions, precipitation has large importance for sensitivity change to NH_3 (R^2=0.97) emissions, and RH highly contributes to sensitivity change to aromatics emissions (R^2=0.68). With respect to transport from upwind regions of Eastern China, wind speed, RH, and PBL height have crucial impacts on sensitivity changes of $PM_{2.5}$ to emission sources. Although these results can explain meteorological impacts to domestic sources with good R^2 (0.41−0.97), these would be insufficient to explain meteorological impacts to upwind regions on adjoint analysis due to moderate R^2 (0.31−0.57).

Equation (18) $$Impact_{i,n} \equiv \frac{\triangle \lambda_i}{\triangle x_{i,n}} * LMG(x_{i,n})\,[\%p]$$

Table 4. Calculated meteorological impacts (%p) on sensitivity of $PM_{2.5}$ to domestic sources using **Equation (18)**. GRIMs shows larger values of upper six variables (RH, Wind speed, SLP, PBL height, Precipitation, and U wind), and smaller values of other three variables (Temperature, Cloud fraction, and V wind) than GEOS-FP.

	NO_x	SO_2	NH_3	BC	OC	AROM	Total (%p)
RH (%p %$^{-1}$)	-0.2	+0.3	+0.2	+0.1	+0.1	+0.6	+1.1
Wind speed (%p m^{-1} s)	-1.8 ±0.4	+0.4 ±0.1	+0.2 ±0.2	+0.1	+0.1	+0.1 ±0.1	-0.9 ±0.7
SLP (%p hPa^{-1})	-0.5 ±0.1	-0.1	+0.3	+0.1	+0.1	+0.3	+0.2 ±0.1
PBL height (%p km^{-1})	-0.1	-0.2	-0.1	0	0	0	-0.4
Precipitation (%p mm^{-1} day)	-1.3 ±0.2	+0.1 ±0.1	+0.3 ±0.1	+0.3	+0.4	+0.2	0 ±0.4
U wind (%p rad^{-1})	-0.5 ±0.5	+0.5 ±0.2	+0.2 ±0.2	+0.3 ±0.1	+0.3 ±0.1	+0.4 ±0.1	+1.2 ±1.2
Temperature (%p K^{-1})	+6.7 ±0.7	-1.0 ±0.2	-0.2 ±0.3	-0.2 ±0.1	-0.2 ±0.1	-0.8 ±0.2	+4.3 ±1.6
Cloud fraction (%p %$^{-1}$)	+0.2 ±0.1	-0.1	-0.3	-0.1	-0.1	-0.1	-0.5 ±0.1
V wind (%p rad^{-1})	-0.6 ±0.5	+0.1 ±0.2	+0.3 ±0.2	0 ±0.1	0 ±0.1	0 ±0.1	-0.2 ±1.2
Total (%p)	+1.9 ±2.5	-0.4 ±0.8	+0.9 ±1.0	+0.6 ±0.3	+0.7 ±0.3	+0.7 ±0.5	

Meteorological effects for sensitivity of $PM_{2.5}$ to domestic sources are quantified by **Equation (18)** and its result is in **Table 4**. RH, wind speed, Sea level pressure, PBL height, precipitation, and U wind with red arrow sign are variables which values in GRIMs are larger than GEOS-FP. On the contrary, temperature, cloud fraction, and V wind with blue arrow sign are variables which values in GRIMs are smaller than GEOS-FP. As examples for interpretation, 1% increase of RH induces more contribution of domestic aromatics emissions to 0.6%p, on the other hand, 1K decrease of temperature results in more contribution of domestic NO_x emissions to 6.7%p. In result, domestic emission sources are most sensitive to temperature, U wind, and RH changes. However, meteorological impacts to sensitivities of $PM_{2.5}$ emission sources from upwind regions in Eastern China are not dealt due to low R^2 as mentioned before.

Chapter 6. Summary

The emissions and sources of $PM_{2.5}$ in different regions of South Korea during the KORUS-AQ campaign were investigated using a GEOS-Chem adjoint model. To improve the source attribution estimates, updated KORUS ver.5.0 anthropogenic emission inventory and SOA formation scheme from aromatic species were included in the model. The model performance was validated using observation data from six ground sites (Bangnyung, Bulkwang, Gwangju, Jeju, Olympic park, and Ulsan). The model overestimates nitrate (NMB: 33%) and underestimates sulfate (NMB: −16%), ammonium (NMB: −8%), and OA (NMB: −30%). However, the updated SOA scheme improves OA simulation from −59% to −30% and PM2.5 simulation from −37% to −27%. Adjoint sensitivity analysis was conducted by calculating the contribution of the source regions and emissions to the $PM_{2.5}$ concentration in South Korea during four meteorological periods: dynamic weather, stagnant, extreme pollution, and blocking pattern periods. Domestic sources show the highest contribution during the dynamic weather (73%), stagnant (58%), and blocking pattern (63%) periods. However, the Chinese region contributes about 57% during the extreme pollution period due to enhanced transport. Considering emission sources, $PM_{2.5}$ is most sensitive to NH_3 emissions (38%) because South Korea is verified to be under NH_3-poor conditions through AGR calculations (0.53). The contributions OC (18%), aromatics (14%), SO_2 (11%), NO_x (10%), and BC (9%)

emissions follow in that order. However, there are uncertainties about the meteorological data used in the model; thus, further adjoint analysis was conducted using GRIMs meteorological data. GRIMs shows lower temperature and higher RH in South Korea, which are favorable for the chemical reactions of nitrate. The calculated AGR (0.75) also indicates NH_3-poor condition in South Korea. Thus, the adjoint analysis using GRIMs shows more contribution of NH_3 (40%) and NO_x (11%) than that using GEOS-FP. Additionally, meteorological effects on the adjoint analysis were confirmed by using LMG method, and it suggests that temperature and RH are leading factor for sensitivity changes of SO_2, NO_x, and aromatics emissions and precipitation largely contributes to sensitivity changes of NH_3 emissions. With respect to transport from upwind regions of Eastern China, wind speed, RH, and PBL height shows large importance. Next, these effects are quantified. Domestic emission sources are most sensitive to temperature, U wind, RH changes.

In this study, we focused on improving the source attribution estimates of $PM_{2.5}$ in South Korea during KORUS-AQ. This was achieved using an updated anthropogenic emission inventory of KORUS ver.5.0 and the SOA formation scheme from aromatics. Additionally, regional contributions are highly dependent on meteorological conditions; therefore, meteorological effects were analyzed and confirmed using GRIMs meteorological data and by relative importance using LMG method. However, this study cannot represent all of $PM_{2.5}$ circumstances around South Korea, therefore, there is a need for further studies in other seasons such as winter and summer to develop more effective air quality policies. Furthermore, the effects of COVID-19 on source

attributions with respect to global and regional changes in the emission of $PM_{2.5}$ should be investigated.

Bibliography

Bey, Isabelle & Jacob, Daniel & Yantosca, Robert & Logan, Jennifer & Field, Brendan & Fiore, Arlene & Li, Qin-Bin & Liu, Hongyu & Mickley, Loretta & Schultz, Martin. 2001. Global Modeling of Tropospheric Chemistry with Assimilated Meteorology: Model Description and Evaluation. Journal of Geophysical Research: Atmospheres. 106. 23,073-23,095.

Bouwman, Alexander & Lee, David & Asman, Willem A.H. & Dentener, Frank & Van der Hoek, Klaas & Oliver, Jos. 1997. A global high-resolution inventory for ammonia. Global Biogeochemical Cycles, 11, 561-587.

Brook, R. D., Rajagopalan, S., Pope, C. A., 3rd, Brook, J. R., Bhatnagar, A., Diez-Roux, A. V., Holguin, F., Hong, Y., Luepker, R. V., Mittleman, M. A., Peters, A., Siscovick, D., Smith, S. C., Jr, Whitsel, L., Kaufman, J. D., & American Heart Association Council on Epidemiology and Prevention, Council on the Kidney in Cardiovascular Disease, and Council on Nutrition, Physical Activity and Metabolism (2010). Particulate matter air pollution and cardiovascular disease: An update to the scientific statement from the American Heart Association. *Circulation*, *121*(21),2331-2378. https://doi.org/10.1161/CIR.0b013e3181dbece1.

Capps, S. L., Henze, D. K., Hakami, A., Russell, A. G., and Nenes, A.: ANISORROPIA: the adjoint of the aerosol thermodynamic model ISORROPIA, Atmos. Chem. Phys., 12,

527-543, https://doi.org/10.5194/acp-12-527-2012, 2012.

Choi, Jong-Kyu & Heo, Jongbae & Ban, Soo-Jin & Yi, Seung-Muk & Zoh, Kyung-Duk. 2013. Source apportionment of PM2.5 at the coastal area in Korea. The Science of the total environment. 447. 370-380.

Choi, Jinkyul & Park, Rokjin & Lee, Hyung-Min & Lee, Seungun & Jo, Duseong & Jeong, Jaein & Henze, Daven & Woo, Jung-Hun & Ban, Soo-Jin & Lee, Min-Do & Lim, Cheol-Soo & Park, Mi-Kyung & Shin, Hye & Cho, Seogju & Peterson, David & Song, Chang-Keun. (2019). Impacts of local vs. trans-boundary emissions from different sectors on PM2.5 exposure in South Korea during the KORUS-AQ campaign. Atmospheric Environment. 203. 196-205.

Fountoukis, C. and Nenes, A.: ISORROPIA II: a computationally efficient thermodynamic equilibrium model for K^+-Ca^{2+}-Mg^{2+}-NH_4^+-Na^+-SO_4^{2-}-NO_3^--Cl^--H_2O aerosols, Atmos. Chem. Phys., 7, 4639-4659, https://doi.org/10.5194/acp-7-4639-2007, 2007.

Goldberg, D. L., Saide, P. E., Lamsal, L. N., de Foy, B., Lu, Z., Woo, J.-H., Kim, Y., Kim, J., Gao, M., Carmichael, G., and Streets, D. G.: A top-down assessment using OMI NO_2 suggests an underestimate in the NO_x emissions inventory in Seoul, South Korea, during KORUS-AQ, Atmos. Chem. Phys., 19, 1801-1818, https://doi.org/10.5194/acp-19-1801-2019, 2019.

Groemping, U. (2006). Relative Importance for Linear Regression in R: The Package relaimpo. *Journal of Statistical Software, 17*(1), 1-27. doi:http://dx.doi.org/10.18637/jss.v017.i01.

Guenther, A., Karl, T., Harley, P., Wiedinmyer, C., Palmer, P. I., and Geron, C.: Estimates of global terrestrial isoprene emissions using MEGAN (Model of Emissions of Gases and Aerosols from Nature), Atmos. Chem. Phys., 6, 3181-3210, https://doi.org/10.5194/acp-6-3181-2006, 2006.

Henze, D. K., Hakami, A., and Seinfeld, J. H.: Development of the adjoint of GEOS-Chem, Atmos. Chem. Phys., 7, 2413-2433, https://doi.org/10.5194/acp-7-2413-2007, 2007.

Heo, J.-B., Hopke, P. K., and Yi, S.-M.: Source apportionment of $PM_{2.5}$ in Seoul, Korea, Atmos. Chem. Phys., 9, 4957-4971, https://doi.org/10.5194/acp-9-4957-2009, 2009.

Hodzic, A., Kasibhatla, P. S., Jo, D. S., Cappa, C. D., Jimenez, J. L., Madronich, S., and Park, R. J.: Rethinking the global secondary organic aerosol (SOA) budget: stronger production, faster removal, shorter lifetime, Atmos. Chem. Phys., 16, 7917-7941, https://doi.org/10.5194/acp-16-7917-2016, 2016.

Hong, SY., Park, H., Cheong, HB. *et al.* The Global/Regional Integrated Model system (GRIMs). *Asia-Pacific J Atmos Sci* 49, 219-243 (2013). https://doi.org/10.1007/s13143-013-0023-0.

Hou, X, Yim, S H L, Chan, C K, & Dong, G H (Mar 2019). Impacts of transboundary air pollution and local emissions on PM_{25} pollution in the Pearl River Delta region of China and the public health, and the policy implications. Environmental Research Letters, 14(3), 10. doi:101088/1748-9326/aaf493.

Hudman, R. & Jacob, Daniel & Turquety, Solene & Leibensperger, Eric & Murray, Lee & Wu, Shunquan & Gilliland, Alice & Avery, Melody & Brune, W. & Cohen, R. & Dibb, J. & Flocke, F. & Fried, A. & Holloway, John & Neuman, Jonathan & Orville, R. & Perring, A. & Ren, Xinrong & Wooldridge, Paul. (2007). Surface and Lightning Sources of Nitrogen Oxides over the United States: Magnitudes, Chemical Evolution, and Outflow. Journal of Geophysical Research. 112. D12S05.

Jeon, W.-B., Lee, H. W., Lee, S.-H., Park, J.-H., & Kim, H.-G. (2014). Numerical Study on the Characteristics of High PM2.5Episodes in Anmyeondo Area in 2009. *Journal of Environmental Science International*, *23*(2), 249-259. https://doi.org/10.5322/jesi.2014.23.2.249.

Jeong, Ju-Hee & Shon, Zang-Ho & Kang, Minsung & Kim, Yoo-Keun & Park, Jinsoo & Kim, Hyunjae. (2017). Comparison of source apportionment of PM2.5 using receptor models in the main hub port city of East Asia: Busan. Atmospheric Environment. 148. 115-127.

Fenger, Jes. (2009). Air pollution in the last 50 years - From

local to global. Atmospheric Environment. 43. 13-22.

Jerrett, M., Burnett, R. T., Pope, C. A., 3rd, Ito, K., Thurston, G., Krewski, D., Shi, Y., Calle, E., & Thun, M. (2009). Long-term ozone exposure and mortality. *The New England journal of medicine*, *360*(11), 1085-1095. https://doi.org/10.1056/NEJMoa0803894.

Jo, D., Park, R., Kim, M., Spracklen, D., 2013. Effects of chemical aging on global secondary organic aerosol using the volatility basis set approach. Atmos. Environ. 81, 230-244.

Jo, Yu-Jin & Lee, hyo-jung & Jo, Hyun-Young & Woo, Jung-Hun & Kim, Younha & Lee, Taehyoung & Heo, Gookyoung & Park, Seung-Myung & Jung, Donghee & Park, Jihoon & Kim, Cheol-Hee. 2020. Changes in inorganic aerosol compositions over the Yellow Sea area from impact of Chinese emissions mitigation. Atmospheric Research. 240. 104948.

Kang, C.-M., Lee, H.S., Kang, B.-W., Lee, S.-K., Sunwoo, Y., 2004. Chemical characteristics of acidic gas pollutants and PM2.5 species during hazy episodes in Seoul, South Korea. Atmos. Environ. 38, 4749-4760.

Kim, B.-U., Bae, C., Kim, H.C., Kim, E., Kim, S., 2017a. Spatially and Chemically Resolved Source Apportionment Analysis: Case Study of High Particulate Matter Event. Atmospheric Environment. 162. 55-70.

Kim, E., Bae, C., Kim, H.C., Cho, J.H., Kim, B.U., Kim, S., 2017b. Regional contributions to particulate matter concentration in the Seoul metropolitan area, Korea: seasonal variation and sensitivity to meteorology and emissions inventory. Atmos. Chem. Phys. 17, 10315-10332, https://doi.org/10.5194/acp-17-10315-2017, 2017.

Kim, H.-S., Huh, J.-B., Hopke, P.K., Holsen, T.M., Yi, S.-M., 2007. Characteristics of the major chemical constituents of PM2.5 and smog events in Seoul, Korea in 2003 and 2004. Atmos. Environ. 41, 6762-6770.

Krewski, D., Jerrett, M., Burnett, R. T., Ma, R., Hughes, E., Shi, Y., Turner, M. C., Pope, C. A., 3rd, Thurston, G., Calle, E. E., Thun, M. J., Beckerman, B., DeLuca, P., Finkelstein, N., Ito, K., Moore, D. K., Newbold, K. B., Ramsay, T., Ross, Z., Shin, H., … Tempalski, B. (2009). Extended follow-up and spatial analysis of the American Cancer Society study linking particulate air pollution and mortality. *Research report (Health Effects Institute)*, (140), 5-136.

Laden, Francine & Schwartz, Joel & Speizer, Frank & Dockery, Douglas. (2006). Reduction in Fine Particulate Air Pollution and Mortality: Extended Follow-up of the Harvard Six Cities Study. American journal of respiratory and critical care medicine. 173. 667-72.

Lamb, KD, Perring, AE, Samset, B, Peterson, D, Davis, S, Anderson, BE, Beyersdorf, A, Blake, DR, Campuzano-Jost, P,

Corr, CA, Diskin, GS, Kondo, Y, Moteki, N, Nault, BA, Oh, J, Park, M, Pusede, SE, Simpson, IJ, Thornhill, KL, Wisthaler, A, Schwarz, JP. 2018. Estimating source region influ- ences on black carbon abundance, microphysics, and radiative effect observed over South Korea. Journal of Geophysical Research: Atmospheres 123(23): 13,527-13,548.

Larkin, A., van Donkelaar, A., Geddes, J. A., Martin, R. V., & Hystad, P. (2016). Relationships between Changes in Urban Characteristics and Air Quality in East Asia from 2000 to 2010. *Environmental science & technology*, *50*(17), 9142-9149. https://doi.org/10.1021/acs.est.6b02549

Lee, H.-M., Park, R.J., Henze, D.K., Lee, S., Shim, C., Shin, H.-J., Moon, K.-J., Woo, J.-H., 2017. Source attribution for Seoul in May from 2009 to 2013 using GEOS-Chem and its adjoint model. Environ. Pollut. 221, 377-384.

Lepeule, J., Laden, F., Dockery, D., & Schwartz, J. (2012). Chronic exposure to fine particles and mortality: an extended follow-up of the Harvard Six Cities study from 1974 to 2009. *Environmental health perspectives*, *120*(7), 965-970. https://doi.org/10.1289/ehp.1104660.

Lim, S. S., Vos, T., Flaxman, A. D., Danaei, G., Shibuya, K., Adair-Rohani, H., Amann, M., Anderson, H. R., Andrews, K. G., Aryee, M., Atkinson, C., Bacchus, L. J., Bahalim, A. N., Balakrishnan, K., Balmes, J., Barker-Collo, S., Baxter, A., Bell, M. L., Blore, J. D., Blyth, F., … Memish, Z. A. (2012). A comparative risk assessment of burden of disease and injury

attributable to 67 risk factors and risk factor clusters in 21 regions, 1990-2010: a systematic analysis for the Global Burden of Disease Study 2010. *Lancet (London, England)*, *380*(9859), 2224-2260.
https://doi.org/10.1016/S0140-6736(12)61766-8.

Liu, H., Jacob, D.J., Bey, I., Yantosca, R.M., 2001. Constraints from 210Pb and 7Be on wet deposition and transport in a global three-dimensional chemical tracer model driven by assimilated meteorological fields. J. Geophys. Res.: Atmosphere 106, 12,109-12,128.

LTP, 2019. Summary Report of the 4th stage (2013- 2017) LTP Project.

Murray, L.T., Jacob, D.J., Logan, J.A., Hudman, R.C., Koshak, W.J., 2012. Optimized regional and interannual variability of lightning in a global chemical transport model constrained by LIS/OTD satellite data. J. Geophys. Res.: Atmosphere 117.

Miyazaki, K., Sekiya, T., Fu, D., Bowman, K.W., Kulawik, S.S., Sudo, K., Walker, T., Kanaya, Y., Takigawa, M., Ogochi, K., Eskes, H., Boersma, K.F., Thompson, A.M., Gaubert, B., Barre, J., Emmons, L.K., 2019, Balance of emission and dynamical controls on ozone during KORUS-AQ from multi-constituent satellite data assimilation, JGR Atmospheres 124, 387-413.

Ng, N. L., Kroll, J. H., Chan, A. W. H., Chhabra, P. S., Flagan, R. C., and Seinfeld, J. H.: Secondary organic aerosol formation

from *m*-xylene, toluene, and benzene, Atmos. Chem. Phys., 7, 3909-3922, https://doi.org/10.5194/acp-7-3909-2007, 2007.

OECD, 2018. Air Quality and Health: Exposure to PM2.5 Fine Particles - Countries and Regions.

Pan, Yuzhou & Zhu, Yun & Jang, Jicheng & Wang, Shuxiao & Xing, Jia & Chiang, Pen-Chi & Zhao, Xuetao & You, Zhiqiang & Yuan, Yingzhi. 2020. Source and sectoral contribution analysis of PM2.5 based on efficient response surface modeling technique over Pearl River Delta Region of China. Science of The Total Environment. 737. 139655.

Park, R.J., Jacob, D.J., Chin, M., Martin, R.V., 2003. Sources of carbonaceous aerosols over the United States and implications for natural visibility. J. Geophys. Res.: Atmosphere 108.

Park, R.J., Jacob, D.J., Field, B.D., Yantosca, R.M., Chin, M., 2004. Natural and trans- boundary pollution influences on sulfate-nitrate-ammonium aerosols in the United States: implications for policy. J. Geophys. Res.: Atmosphere 109.

Park, R.J., Jacob, D.J., Kumar, N., Yantosca, R.M., 2006. Regional visibility statistics in the United States: natural and transboundary pollution influences, and implications for the Regional Haze Rule. Atmos. Environ. 40, 5405-5423.

Park, S.S., Kim, Y.J., 2005. Source contributions to fine particulate matter in an urban atmosphere. Chemosphere 59,

217-226.

Pelucchi, C., Negri, E., Gallus, S. *et al.* Long-term particulate matter exposure and mortality: a review of European epidemiological studies. *BMC Public Health* **9,** 453 (2009). https://doi.org/10.1186/1471-2458-9-453.

Peterson, D, Hyer, E, Han, S-O, Crawford, J, Park, R, Holz, R, Kuehn, R, Eloranta, E, Knote, C, Jordan, C, Lefer, B. 2019. Meteorology influencing spring- time air quality, pollution transport, and visibility in Korea. Elementa: Science of the Anthropocene 7: 57.

Pope, C. A., 3rd, Ezzati, M., & Dockery, D. W. (2009). Fine-particulate air pollution and life expectancy in the United States. *The New England journal of medicine*, *360*(4), 376-386. https://doi.org/10.1056/NEJMsa0805646.

Pye, H., Liao, H., Wu, S., Mickley, L.J., Jacob, D.J., Henze, D.K., Seinfeld, J., 2009. Effect of changes in climate and emissions on future sulfate-nitrate-ammonium aerosol le- vels in the United States. J. Geophys. Res.: Atmosphere 114.

Ryou, H.G., Heo, J., Kim, S.Y., 2018, Source apportionment of PM10 and PM2.5 air pollution, and possible impacts of study characteristics in South Korea, Environmental Pollution 240, 963-972.

Sajeev, P., Randall, V.M., Graydon, S., Crystal, L.W., Aaron van,

D., Michael, B., Daven, K.H., Zbigniew, K., Chandra, V., Sarath, K.G., Qiang, Z., 2017. Anthropogenic fugi- tive, combustion and industrial dust is a significant, underrepresented fine particulate matter source in global atmospheric models. Environ. Res. Lett. 12, 044018.

Streets, D.G., Yan, F., Chin, M., Diehl, T., Mahowald, N., Schultz, M., Wild, M., Wu, Y.,Yu, C., 2009. Anthropogenic and natural contributions to regional trends in aerosol optical depth, 1980e2006. Journal of Geophysical Research 114, D00D18.

Turpin, B.J., Lim, H.-J., 2001. Species contributions to PM2. 5 mass concentrations: re- visiting common assumptions for estimating organic mass. Aerosol Sci. Technol. 35, 602-610.

Wang, Jikang & Xu, Jun & He, Youjiang & Chen, Yunbo & Meng, Fan. 2016. Long range transport of nitrate in the low atmosphere over Northeast Asia. Atmospheric Environment. 144.

Wang, Shuxiao & Xing, Jia & Jang, Carey & Zhu, Yun & Fu, Joshua & Hao, Jiming, 2011. Impact Assessment of Ammonia Emissions on Inorganic Aerosols in East China Using Response Surface Modeling Technique. Environmental science & technology. 45. 9293-300.

Wang, Y., Jacob, D.J., Logan, J.A., 1998. Global simulation of tropospheric O3-NO x-hydrocarbon chemistry: 1. Model formulation. J. Geophys. Res.: Atmosphere 103, 10713-10725.

Wesely, M., 1989. Parameterization of surface resistances to gaseous dry deposition in regional-scale numerical models. Atmos. Environ. 23, 1293-1304 1967.

Woo, J.H., Choi, K.C., Kim, H.K., Baek, B.H., Jang, M., Eum, J.H., Song, C.H., Ma, Y.I., Chang, L.S., Yoo, S.H., 2012, Development of an anthropogenic emissions processing system for Asia using SMOKE, Atmospheric Environment 58, 5-13.

Wu, Yiyun & Gu, Baojing & Erisman, Jan Willem & Reis, Stefan & Fang, Yuanyuan & Lu, Xuehe & Zhang, Xiuming. 2016. PM2.5 pollution is substantially affected by ammonia emissions in China. Environmental Pollution. 218. 86-94.

Ye, C., Zhou, X., Pu, D., Stutz, J., Festa, J., Spolaor, M., Tsai, C., Cantrell, C., Mauldin, R.L., Campos, T., 2016. Rapid cycling of reactive nitrogen in the marine boundary layer. Nature 532, 489-491.

Yienger, J., Levy, H., 1995. Empirical model of global soil-biogenic NOχ emissions. J. Geophys. Res.: Atmosphere 100, 11447-11464.

Zhu, L., Henze, D., Bash, J., Jeong, G.-R., Cady-Pereira, K., Shephard, M., Luo, M., Paulot, F., and Capps, S.: Global evaluation of ammonia bidirectional exchange and livestock diurnal variation schemes, Atmos. Chem. Phys., 15, 12823-12843, https://doi.org/10.5194/acp-15-12823-2015, 2015.

국문 초록

최근 대기질에 대한 관심의 증가로 초미세먼지(PM2.5)는 우리나라에서 가장 큰 환경 이슈 중 하나가 되었다. 따라서, 효과적인 대기질 정책 수립을 위한 초미세먼지의 오염원 분석의 중요성이 대두되었다. 본 연구에서는 3차원 전 지구 화학수송모델인 GEOS-Chem 모델과 업데이트된 KORUS ver.5.0의 배출 인벤토리를 사용하였다. 연구 기간인 KORUS-AQ 캠페인은 2016년 5월부터 6월 초까지 수행된 한-미 대기질 합동 연구로, 항공기 및 지상 관측 등을 통해 PM2.5를 포함한 에어로졸과 그 전구 물질에 대한 관측 자료가 수집되었으며, 본 연구에서는 백령도, 불광동, 광주, 제주도, 올림픽공원, 울산의 관측 결과를 바탕으로 모델을 평가하였다. 또한 초미세먼지 모의 성능을 향상시키기 위해 최근의 VBS 연구 결과를 화학 스킴에 적용해 이차유기에어로졸(SOA)의 모의를 향상시켰다. 그 결과 화학종 및 초미세먼지 모의가 향상되었음을 확인하였다. 이후 우리나라 초미세먼지에 대한 오염원 분석을 진행하였으며, 각각의 기상 패턴에 따라 4개의 기간으로 나누어 연구를 진행하였다. 고기압의 영향권 내에 한반도가 위치하여 대기가 정체된 Stagnant 기간에는 국내 영향이 58%, 중국 영향이 36%를 차지하였으며 국내의 NH_3(16%)와 OC(13%)가 높은 기여도를 보였다. 또한 중국으로부터의 수송이 강화되어 대기질 기준을 초과하는 농도의 초미세먼지가 관측된 Extreme pollution 기간에는 국내 영향이 38%, 중국 영향이 57%를 차지하였으며 중국의 NH_3(14%)와 NO_x(11%), 국내의 NH_3(12%)가 높은 기여도를 보였다. KORUS-AQ 기간 동안 배출원 중 NH_3의 기여도가 NO_x와 SO_2에 비해 상당함을 확인할 수 있었는데, 이는 우리나라가 NH3-poor 조건에 있음을 AGR 계산을 통해 밝혀내었다. 추가적으로 기상장의 불확실성에 기인한 영향을 분석하기 위한 연구를 진행하였다. 모델에 의해 모의된 GRIMs기상장을 사용하였으며, 전체적으로 GEOS-FP에 비해 낮은 기온과 높은 상대습도를 보였다. 이는

Nitrate 에어로졸 형성에 유리한 조건으로, 오염원 분석 결과에서 또한 더 높은 NO_x의 기여도 (11%)를 보였다. 이와 동시에 우리나라는 여전히 NH_3-poor 조건에 속하여 NH_3의 기여도 (40%) 또한 높음을 확인하였다. 이후 오염원 분석에 대한 기상 변수들의 영향을 정량화하기 위해 다중선형회귀분석 및 LMG 방법을 사용하였으며, 우리나라의 배출원은 기온, 상대습도 및 강수량에 민감하며 풍상지역인 중국의 경우 풍속과 상대습도, 행성경계층 등에 민감함을 확인하였다.

주요어 : KORUS ver.5.0 인벤토리, SOA 화학스킴, KORUS-AQ, 오염원 분석, AGR, LMG.
학 번 : 2019-29383